Available online at www.sciencedirect.com
SCIENCE DIRECT®
ELSEVIER
Palaeogeography, Palaeoclimatology, Palaeoecology 237 (2006) 293–304
PALAEO
www.elsevier.com/locate/palaeo

Coherence between solar activity and the East Asian winter monsoon variability in the past 8000 years from Yangtze River-derived mud in the East China Sea

Shangbin Xiao [a,b,*], Anchun Li [a], J. Paul Liu [c], Muhong Chen [b], Qiang Xie [b], Fuqing Jiang [a], Tiegang Li [a], Rong Xiang [b], Zhong Chen [b]

[a] *Institute of Oceanology, Chinese Academy of Sciences, Qingdao 266071, China*
[b] *South China Sea Institute of Oceanology, Chinese Academy of Sciences, Guangzhou 510301, China*
[c] *Department of Marine, Earth and Atmospheric Sciences, North Carolina State University, Raleigh, NC 27695, USA*

Received 23 May 2005; received in revised form 22 November 2005; accepted 5 December 2005

Abstract

AMS^{14}C dating and grain-size analysis for Core PC-6, located in the middle of a mud area on the inner shelf of the East China Sea (ECS), were used to rebuild the Holocene history of the East Asian winter monsoon (EAWM). The 7.5-m core recorded the history of environmental changes during the postglacial transgression. The core's mud section (the upper 450 cm) has been formed mainly by suspended sediment delivered from the Yangtze River mouth by the ECS Winter Coastal Current (ECSWCC) since 7.6 kyr BP. Using a mathematical method called "grain size vs. standard deviation", we can divide the Core PC-6's grain-size distribution into two populations at about 28 μm. The fine population (<28 μm) is considered to be transported by the ECSWCC as suspended loads. Content of the fine population changes little and represents a stable sedimentary environment in accord with the present situation. Thus, variation of mean grain-size from the fine population would reflect the strength of ECSWCC, which is mainly controlled by the East Asian winter monsoon.

Abrupt increasing mean grain size in the mud section is inferred to be transported by sudden strengthened ECSWCC, which was caused by the strengthened EAWM. Thus, the high resolution mean grain-size variation might serve as a proxy for reconstruction of the EAWM. A good correlation between sunspot change and the mean grain-size of suspended fine population suggests that one of the primary controls on centennial- to decadal-scale changes of the EAWM in the past 8 ka is the variations of sun irradiance, i.e., the EAWM will increase in intensity when the number of sunspots decreases. Spectral analyses of the mean grain-size time series of Core PC-6 show statistically significant periodicities centering on 2463, 1368, 128, 106, 100, 88-91, 76-78, and 70-72 years. The EAWM and the East Asian summer monsoon (EASM) agree with each other well on these cycles, and the East Asian Monsoon (EAM) and the Indian Monsoon also share in concurrent cycles in Holocene, which are in accord with the changes of the sun irradiance.

Keywords: Solar irradiance; East Asian Monsoon; Holocene; Spectral analyses; East China Sea; Grain-size

* Corresponding author. Institute of Oceanology, Chinese Academy of Sciences, Qingdao 266071, China. Tel.: +86 532 82898521; fax: +86 532 82898612.
E-mail addresses: shangbinx@163.com (S. Xiao), acli@ms.qdio.ac.cn (A. Li).

0031-0182/$ - see front matter © 2005 Elsevier B.V. All rights reserved.
doi:10.1016/j.palaeo.2005.12.003

1. Introduction

The East Asian Monsoon (EAM) not only greatly impacts and controls China's climate (Zhang and Lin, 1992), but also plays a significant role in the global climate system (Yasunari and Seki, 1992). The summer monsoon brings a warm moist maritime air/rainfall from low-latitude oceans to the continent. In contrast, the winter monsoon brings cold and dry air out of north-central Asia. The EAM not only affects the circulatory flow, weather and climate changes of East Asia, but also makes the global holding up heat source and divergence centre move eastward, and even affects the weather and climate of North America by remote correlation (Ding, 1996).

The EAWM is the active factor in the East Asian winter–summer monsoon system (Ding et al., 1995). In the Northern Hemisphere's winter seasons, strong temperature contrast between the colder Eurasian continent and surrounding oceans causes surface high pressure cells over the Mongolia–Siberia regions. The coupling of Mongolian–Siberian high pressure cells with the low pressure cells over the Northwest Pacific Ocean (Aleutian Low), the Australia–New Guinea regions (Equatorial Lows), and the African continent (African Low) can produce vigorous northwesterly and northeasterly geostrophic flows over eastern and southern Asia. These flows are, respectively known as the northwesterly monsoon and the northeasterly monsoon (Zhang and Lin, 1992). The northwesterly monsoonal air reaching northern China only flows over land, so it is extremely dry and cold (Trewartha, 1981). The northeasterly monsoon current can frequently push northerly and northeasterly low-level cold air from Siberia through central China as far south as the equatorial South China Sea and the Indonesian Seas, and result in rapid temperature dropping (Chang and Lau, 1980; Chu and Parks, 1984). Meteorological observations (Chen et al., 1991) showed that the low-level northerly and northeasterly air currents originated from high latitudes of the Northern Hemisphere, can occasionally flow across the Equator around 105°E, and then merge with the Australian summer monsoon (Chen et al., 1991; Ding et al., 1995).

Grain-size and magnetic susceptibility of the Chinese loess have been regarded as proxies of the EAWM and EASM, respectively over long-time scales (An et al., 1991; Stephen and An, 1995). However, using loess deposits to study the high-resolution climate changes during the Holocene, in centennial or even shorter time scales is difficult due to its low sedimentation rate. Thus, ice core, peat, pollen, tree ring, lacustrine and deep sea sediments, as well as cave carbonate deposits have been gaining preference as high-resolution methods for studying Chinese paleoclimate and the EAM. However, these land-based, high-resolution records are mainly limited to the study of the EASM or the whole climatic changes within the Holocene period. The latest report showed that higher solar irradiance corresponded to a stronger EASM (Wang et al., 2005). In this paper, we report the mean grain-size distribution in sediment cores on the ECS inner shelf as a high-resolution proxy to discuss variation of the EAWM in the last 8 kyr, and determine its periodicities and forcing mechanisms.

2. Regional setting

With a sediment discharge rate of 4.8×10^8 t/a, huge amounts of sediment have accumulated in the estuary and offshore of the Yangtze River, especially at its southern side (Milliman and Meade, 1983). A major feature of the ECS Coastal Current (ECSCC) is its seasonally changing flow path. The ECSCC flows northward in summer owing to the southeast monsoon, and flows southward in winter owing to the prevailing north wind (Qin et al., 1987; Su, 2001) (Fig. 1 (a)). The modern surface mud on the inner shelf of ECS, so-called "ECS inner shelf mud", is mainly derived from suspended sediments from the Yangtze River, and transported southward by the winter coastal current (Milliman et al., 1989; Su et al., 1989; Gu et al., 1997; Guo et al., 1999; Sun et al., 2000; Hu and Yang, 2001; Xiao et al., 2005a; Liu et al., in press) (Fig. 1 (b)). The latest studies suggested that nearly 50% of Yangtze River-derived sediment had been delivered to the ECS, of which approximately 30% had been transported southward along the Zhejiang and Fujian coasts by the ECSCC (Liu et al., in press). High resolution seismic profiling and AMS^{14}C dating indicate that this extensive distributed mud mainly formed in the past 7600 yr after postglacial sea level reached its mid-Holocene highstand (Liu et al., in press; Xiao et al., 2005c).

Sediment accumulation rate in the Yangtze estuary increased one time around 2000 yr BP, reflecting the evolution of the estuary and increased land erosion due to human activities, such as farming and deforestation (Li et al., 2000; Hori et al., 2002; Liu et al., in press). Sediments transported by the Yangtze River were estimated to be about 2.4×10^8 t/yr between 8–2 kyr BP (Hori et al., 2002; Liu et al., in press). The fact that most sediments carried by the Yangtze River are from upstream regions, indicates the precipitation in Qin-

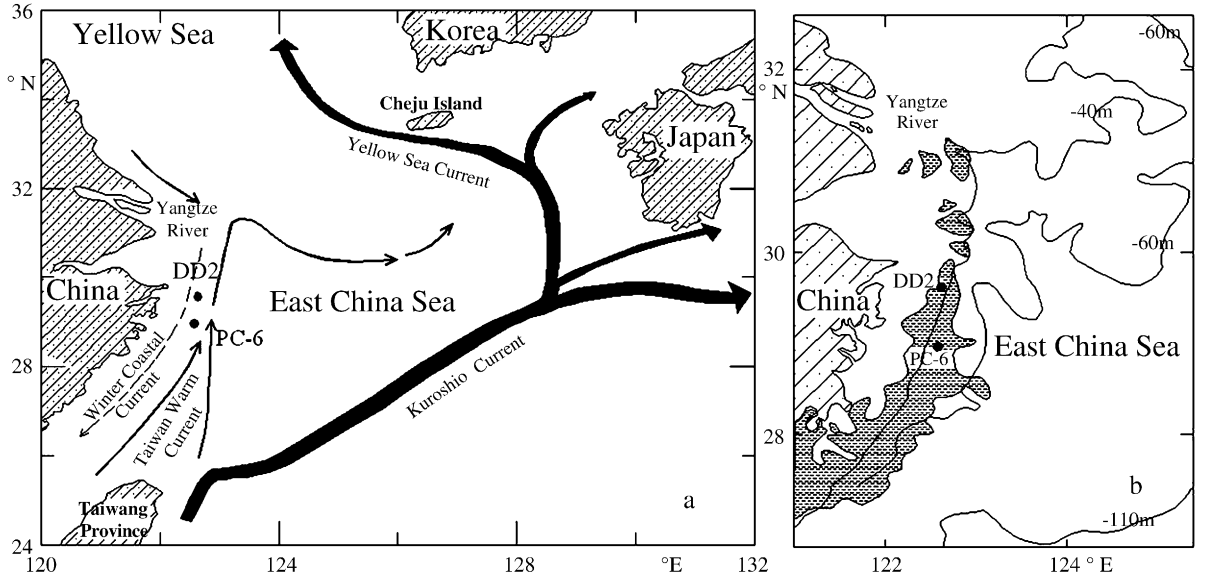

Fig. 1. The studying area, core locations and current systems of the ECS during winter times and distribution of mud on the inner shelf of the ECS. Modified from Qin et al. (1987) and Su (2001).

ghai–Tibet plateau may play a key role in the amount of sediment loads entering the East China Sea (Zhu, 2001). The rainfall in Qinghai–Tibet plateau reached its maximum at about 12 kyr BP, gradually decreased between 12–6 kyr BP, then sharply declined after 6 kyr BP according to paleo-climate model of Community Climate Model (Winkler and Wang, 1993; Saito et al., 2001).

The winter ECSCC flows more rapidly when the winter monsoon strengthens, which results in deposition of coarser grain-size, and vice versa. This phenomenon allows us to use grain-size variability of sediment cores from the coastal mud as a proxy to discuss changes of the EAWM during the Holocene. In our previous work, Core DD2, which is located at the north of the Yangtze River-derived mud on the inner shelf of the ECS, provides a high-resolution record of the EAWM during the last 2 ka. Climatic events disclosed by Core DD2 are well in accordance with Chinese historical documents (Xiao et al., 2005b).

3. Materials and methods

CORE PC-6, 7.5 m in length, is located in the mud area off Zhejiang province coast on the inner shelf of the ECS (122°37.92′E, 29°34.92′N) with a water depth of 56.7 m, and is far away from the Yangtze River estuary (Fig. 1). The core was described in detail and sampled at 2 cm intervals except for the bottom section from 740–750 cm. Samples were pre-processed with excess H_2O_2 ($\varphi = 30\%$) and HCl (3N) successively. Grain size samples were analyzed with a Cilas 940L instrument. Radiocarbon dating was carried out at NOSAMS, Woods Hole Oceanographic Institution. All ^{14}C ages have been calibrated to calendar age using CALIB4.3 software (Stuiver et al., 1998) (Table 1). It is inferred that the age is 7.64 kyr BP (ages used in this paper are cal. ages) at 450 cm where the lower limit of mud section is located (Fig. 2) by assuming a stable sedimentation rate from 350 to 450 cm. The changes of sedimentation rate in Table 1 is well corresponding to that of rainfall in Qinghai–Tibet plateau.

Table 1
^{14}C dating age and sedimentation rate of Core PC-6

Depth/cm	Material	^{14}C age/a BP (1 sigma)	Calendar age/a BP	Depth/cm	Sedimentation rate (cm/ka)	Sample resolution/a
74~76	Mixed benthic Foraminiferas	1830 ± 25	1357 (1329–1392)	0–76	53.69	35.7
178~180		4860 ± 35	5213 (5067–5257)	76–180	26.97	74.2
278~280		6550 ± 35	7046 (6998–7141)	180–280	54.56	36.7
348~350		6960 ± 35	7450 (7421–7486)	280–350	173.27	11.5
428~430		7140 ± 40	7602 (7570–7645)	350–450	540.54	3.8

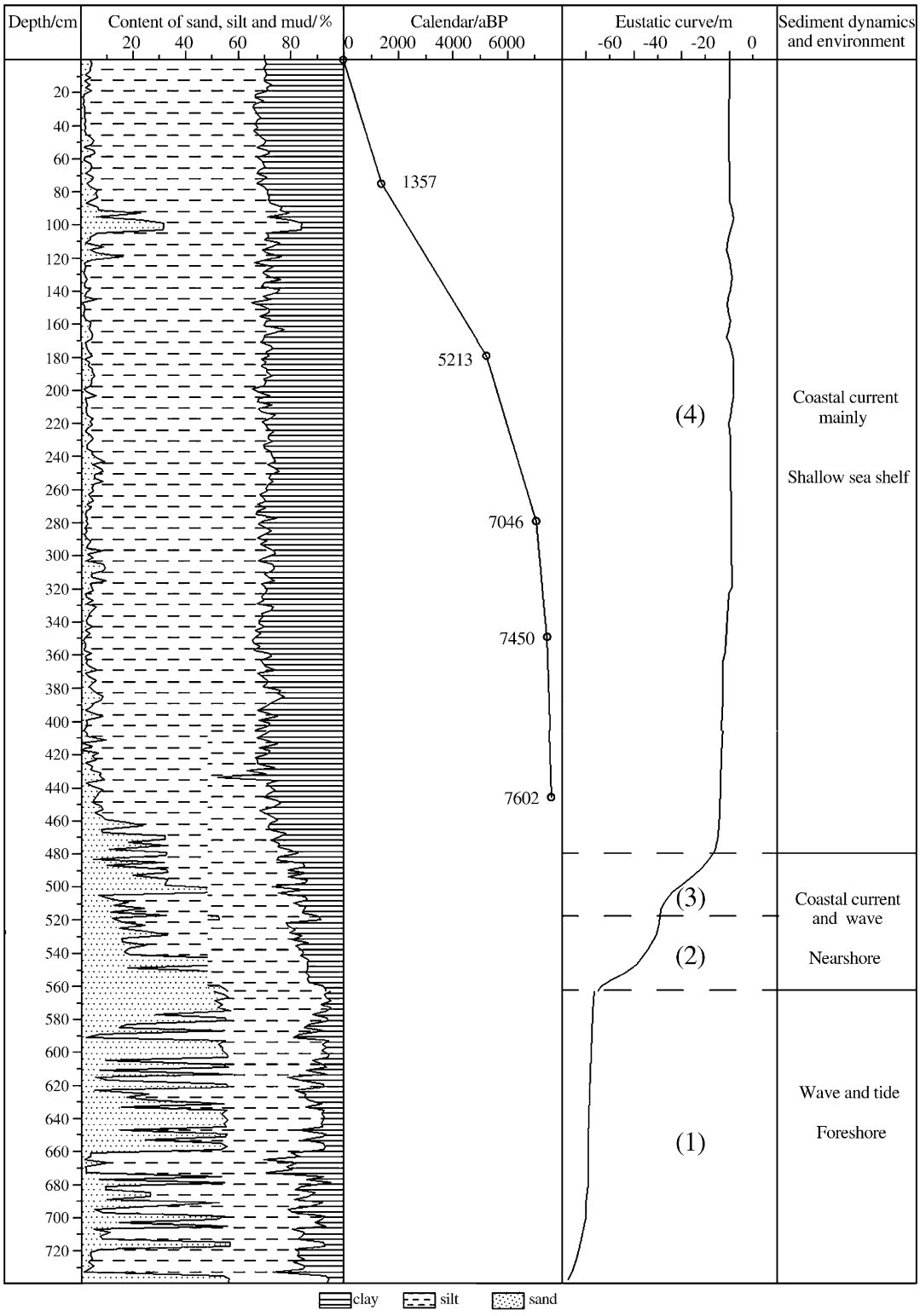

Fig. 2. Chronological strata and sediment dynamics of Core PC–6. The sea level curve is according to Liu et al. (2004), and Liu and Milliman (2004).

4. Grain-size sensitive to sedimentary environments in Core PC-6

4.1. Lithology and sedimentary environment

The core was divided into 3 sections according to its changes in lithology, color, sedimentary structure and stacked pattern of cyclothems (Fig. 2).

The lower section (540–750 cm) is mainly composed of silty sand, with thin interbedding of silty sand and sandy silt, and rich in shell fragments. Sedimentary structures include erosion-filling, bioturbation and so on. Silt content decreases and sand content increases upwardly, which results in coarsing grain-size. This shows inverse grading and appears a sedimentary sequence of shore resulting from transgression, i.e. around 62 m (water depth of 56.7 m plus 5.4 m sediment deposits) below the present sea level. The studies of western Pacific sea-level history show the ECS sea level reached −75 m after melt-water pulse-1A (MWP-1A, 14.3–14.1 kyr BP), and gradually rose to ~60 m before the MWP-1B events (11.5–11.1 kyr BP) (Liu et al., 2004; Liu and Milliman, 2004).

Clearly, the sediment in this section is the result of a slow transgression process (Eustatic curve Section (1) in Fig. 2). The main sedimentary dynamics is wave and tide. These results indicate the foreshore location of sediments within this section.

The middle section (450–540 cm) is mainly composed of light grey sandy silt. Sand content in this section is less than the lower section described above. This section consists of 2 stacked fining upward parasequences of transgression and rapid sea level rise of ~30 and ~25 m (Eustatic curve Section (2) and (3) in Fig. 2). Wave and tide energy in this area decreased with rapid sea level rise, resulting in increasing water depth, and gradually strengthening coastal current. This section belonged to nearshore sediment.

The upper section (0–450 cm) is mainly composed of light grey and taupe clayey silt and clay, and contents of silt and sand change little with the exception of the sandy silt interlayer at 100 cm, which may have resulted from a storm. Sedimentary environment of this section belongs to a shallow sea shelf dominated by the coastal currents, and was formed during a period of high sea level after transgression. The fluctuation of sea level was about 3–4 m (Eustatic curve Section (4) in Fig. 2) in the ECS since the last 7.6 kyr (Liu et al., 2004). No obvious deposition event was observed except at ~100 cm. This indicates a relatively stable sediment environment that extends to present day.

4.2. Grain-size sensitive to sedimentary environments

The upper section of Core PC-6 (mud section) shows little change in grain-size frequency distribution curves (Fig. 3). Mean grain-size, sorting and sharpness are in accord with each other on the whole, illustrating very stable sedimentary dynamics and environment (Fig. 4). In summary, the upper section of Core PC-6 was delivered mainly by the ECSCC with suspended mechanics since 7.6 ka BP.

The pattern of terrigenous sediment transported to the sea is controlled by many factors, which results in

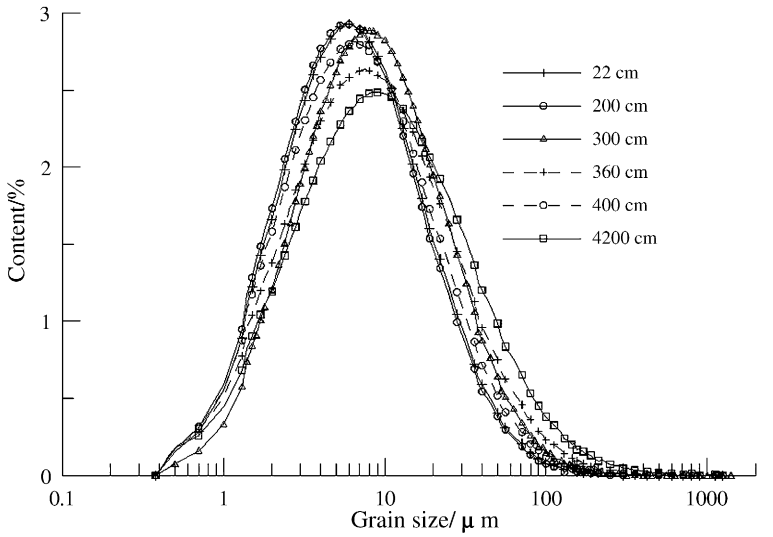

Fig. 3. Grain-size frequency distribution of Core PC-6 samples at different depth.

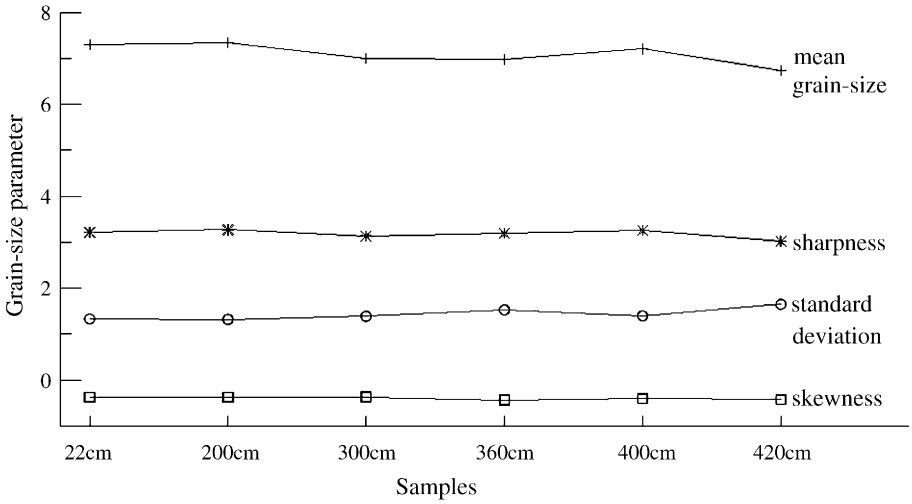

Fig. 4. Comparison of grain-size parameters between samples at different depth of Core PC-6.

selective transport and mixture of sediments from different provenances. Sedimentary succession and grain-size characteristics (such as mode, component and population) in the same environment vary with locations (Gao and Collins, 1998). However, grain-size data in conjunction with important environmental indicators (such as current velocity) vary little (McCave et al., 1995a,b; Moerz and Wolf-Welling, 2001), so we can extract grain-size populations sensitive to environments and their characteristics (such as mode, range of grain-size distribution, content of different populations, etc.) from complex grain-size data to analyze marine sedimentary paleo-environment. This method of using grain-size populations of sediment and their distribution range to trace the sediment transportation processes and changing sedimentary environments was well applied in studies in the Arabian Sea (Prins and Weltje, 1999; Prins et al., 2000a,b), the South China Sea (Boulay et al., 2002), southwestern Africa (Stuut et al., 2002), the Okinawa Trough (Sun et al., 2003) and the shelf of the ECS (Xiao and Li, 2005), the North Pacific (Rea and Hovan, 1995), and Chinese loess (Sun et al., 2002, 2004). Mathematical methods used to partition grain-size populations of sediments are fitting function based on Weibull distribution (Sun et al., 2002, 2004), end-member modeling of grain-size (Prins and Weltje, 1999; Prins et al., 2000a, 2000b; Stuut et al., 2002), and grain-size vs. standard deviation (Boulay et al., 2002; Sun et al., 2003; Xiao and Li, 2005).

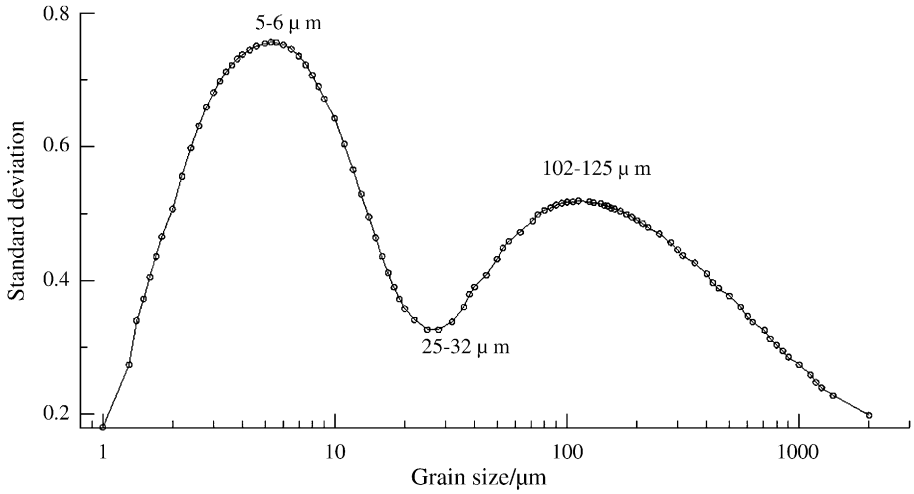

Fig. 5. Standard deviation vs. grain-size of Core PC-6.

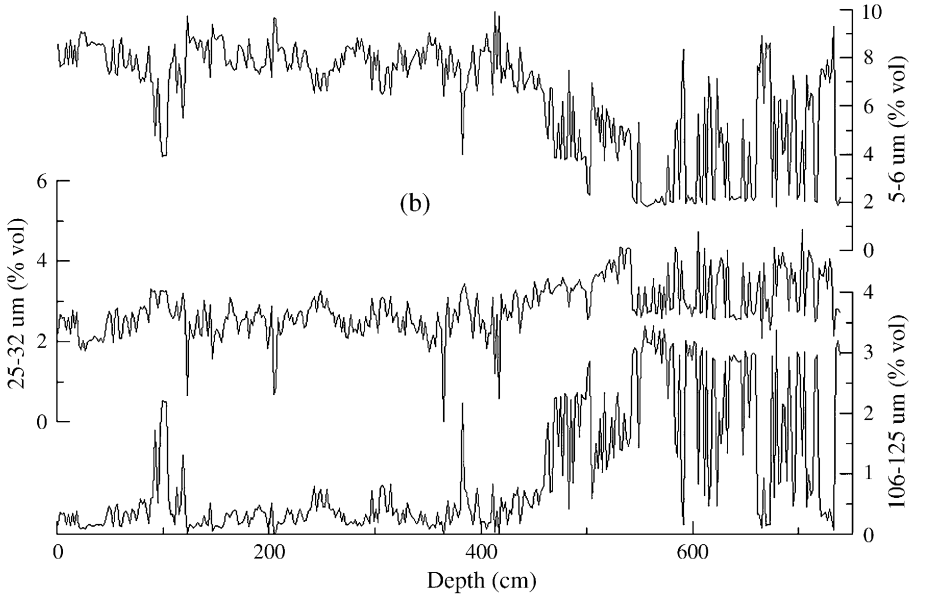

Fig. 6. Variations of the proportion of the grain size classes 5–6, 25–32, and 102–125 μm vs. depth.

Here, we used the "grain-size vs. standard deviation" method to identify the grain size intervals with the highest variability along a sedimentary sequence. Standard deviations were calculated for our 370 samples, for each 100 grain size classes given by the Cilas 940L. Standard deviation values vs. grain size classes are displayed in Fig. 5. Two peaks are observed in this plot, at 5- to 6- and 102- to 125-μm grain size intervals,

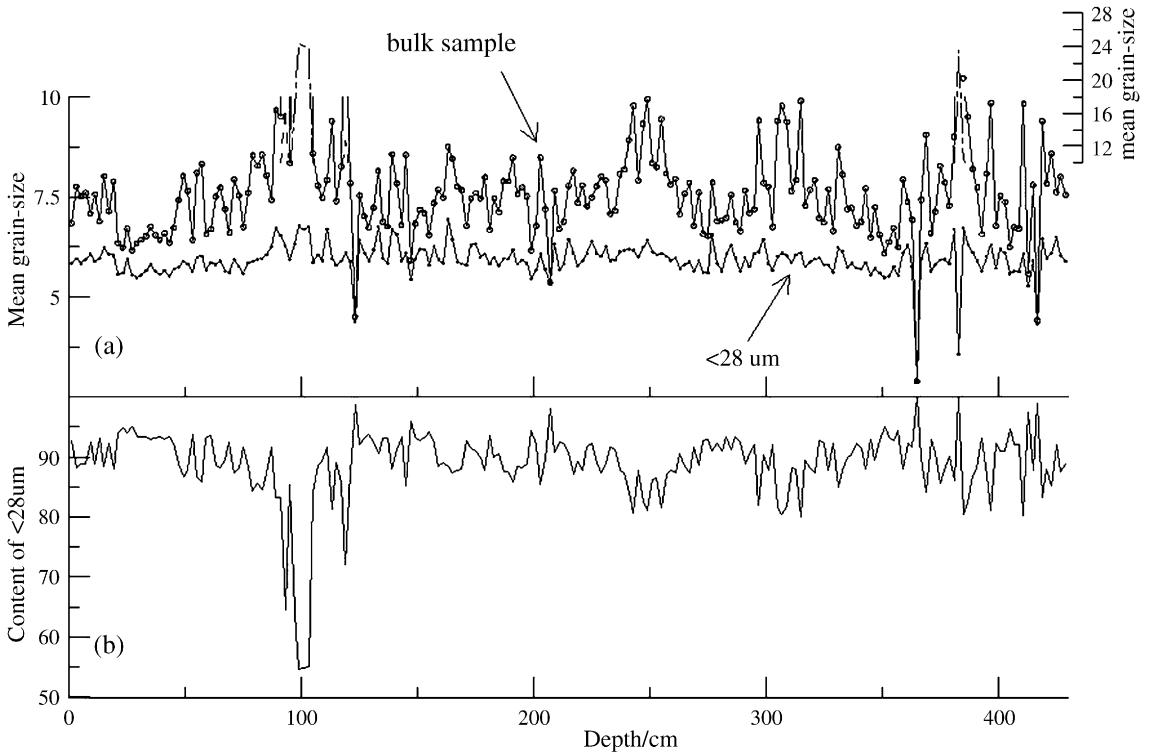

Fig. 7. Vertical variation of mean grain-size and content of fine population of Core PC-6.

respectively. Each of these size classes represents a population of grains with the highest variability through time. On the other hand, the intermediate 25- to 32-μm size class is characterized by low standard deviation values, implying no important changes within this proportion of grain size population in the siliciclastic fraction. This result is confirmed by the variations of the 5- to 6-, 25- to 32-, and 102- to 125-μm size class proportion (percent) through time (Fig. 6). Both the 5- to 6- and 102- to 125-μm grain size populations vary significantly. However, variation in the 25- to 32-μm grain size population was not significant. Long-term fluctuations of the 5- to 6-μm size class distribution are inversely correlated to those of the 102- to 125-μm size class. The 5- to 6- and 102- to 125-μm, are grain-sizes sensitive to different sedimentary environments. The former is sensitive to the coastal current and the latter to wave action (Xiao and Li, 2005).

The content of the fine population (<28 μm) of most samples from the upper section are more than 85% and change little (Fig. 7 (b)), which also suggests a stable sedimentary environment from 7.6 kyr BP to present. Therefore, the upper section can be used to reconstruct a high-resolution paleoenvironment and paleoclimate sequence. Furthermore, the comparison between mean grain-size of populations from bulk samples and <28 μm shows synchronistical change (Fig. 7 (a)). In this paper, only mean grain-size of <28 μm above 450 cm was adopted.

5. Discussion

As stated above, mean grain-size of the suspended population is proportional to the velocity of winter ECSCC, which results from the EAWM. The ΔMG (=mean grain-size of each sample — average grain-size of all samples) of the suspended population was used in Fig. 8 for clarification.

The high temporal resolution of the ΔMG enables comparison with ΔSN (=number of sunspots — number of average sunspots). Fig. 8 shows larger ΔMG well corresponds to small ΔSN except for three periods (marked with shadow). This means the EAWM increased in strength when the number of sunspots decreased.

The intensity of the Indian Monsoon was found to have decreased during periods of solar minima during the last millennium (Agnihotri et al., 2002). The similarity between the ΔMG and ΔSN time series is very strong, especially in the high-resolution interval after ~1600 yr BP and before 5000 yr BP. The parallel evolution of ΔMG and ΔSN seems very unlikely to have occurred by chance. Variation of the ΔMG was attributed to strength changes of the EAWM. The high correlation provides solid evidence that a relationship existed between the EAWM and sun irradiance.

Spectral analysis was widely used to detect hidden periodicities in noisy temporal series derived from stratigraphic sequences. It allowed the variance of a time series to be separated into contributions associated with different time scales, which helped to better understand the physical processes generating the variability recorded in a time series. Spectra of paleoclimatic time series frequently show a continuous decrease of spectral amplitude with increasing frequency ("red-noise") (Schulz and Mudelsee, 2002). The high resolution and dating precision of the grain-size record of Core PC-6 make it possible to perform a reliable frequency analysis. The mean grain-size time series is analyzed here using the REDFIT35 (Schulz and Mudelsee, 2002), which was projected to unevenly spaced time series. Spectral analyses of the grain-size record are given in Fig. 9. It showed statistically significant periodicities centre on 2463, 1368, 456, 397, 280, 237, 173, 140, 128, 111, 106, 100, 88–91, 76–78 and 70–72 years. Most of these cycles are close to the periodicities of the tree-ring $\Delta^{14}C$ record (440, 360, 260, 230, 180, 168, 155, 147, 123, 106, 126 and 88 years), which were assigned to solar modulation (Stuiver and Braziunas, 1993).

On millennial scale, the 1368 years cycle was well in accord with the accepted 1350 years recorded in the North Atlantic (Bond et al., 1997), which was also disclosed in the Okinawa Trough of the ECS (Jian et al., 2000) for Holocene events. The cycle of 2463 years was statistically similar to the 2560 years recorded in the Okinawa Trough (Jian et al., 2000). A ~2500 year's cycle was previously identified in the Camp Century ice core ^{18}O profile (Dansgaar et al., 1984).

On a centennial scale, strong periodical signals of 78, 88–91, 100, 106, 128 and relatively weak 111, 140, 173, 237 years that were disclosed by Core PC-6 agree with a series of centennial precipitation cycles suggested by Spectral analyses of peat $\delta^{13}C$ from Jinchuan, Northeast of China (80, 90, 107, 110, 123, 134, 141, 162, 249 years) during the last 6 ka, which are considered as responses of the sun's activity cycles (Hong et al., 2001). The precipitation and drought in Jinchuan was controlled by the EASM. The 102 and 84 years are suggested as centennial cycles of the EASM during the Holocene according to spectral analysis of U_k^{37} from sediments in the South China Sea (Wang and Sarnthein, 1999). It can be concluded that some cycles of the EAWM and EASM agree with each other on centennial timeframes and their changes are controlled by the same

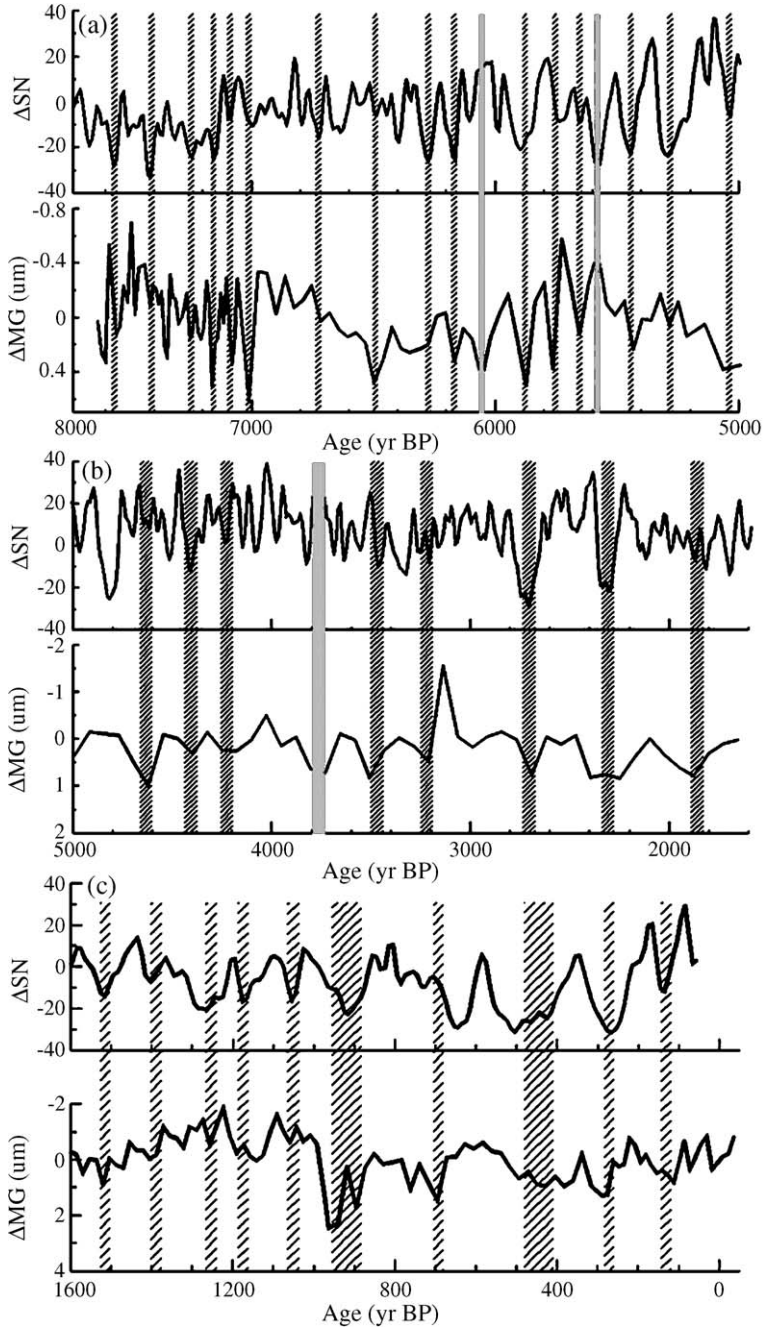

Fig. 8. Profiles of ΔSN and ΔMG from Core PC-6 (a, b), DD2 (c). Owing to Core DD2's higher temporal resolution (about 16 a) than Core PC-6 after 1600 yr BP, ΔMG of the former is used in profile (c) to replace that of the latter. ΔSN Sunspot number was reconstructed by Solanki et al. (2004) based on dendrochronologically dated radiocarbon concentrations (Stuiver et al., 1998); DD2's data are from Xiao et al. (2005b).

factors. The centennial cycles of India Monsoon are inferred to be 71, 80, 89, 105, 120, 151 years based on study of a sediment core from the eastern Arabian Sea dating back to 1200 a BP (Agnihotri et al., 2002). The $\delta^{18}O$ record of stalagmite from Oman showed strong coherence between solar variability and the India Monsoon during the early Holocene (Meff et al., 2001). It appears the EAM and the Indian Monsoon show concurrent cycles during the Holocene, which agree with the cycles of sun irradiance (Stuiver et al., 1991).

Singular spectrum analysis of the surface temperature records for 11 geographical regions in the last 150

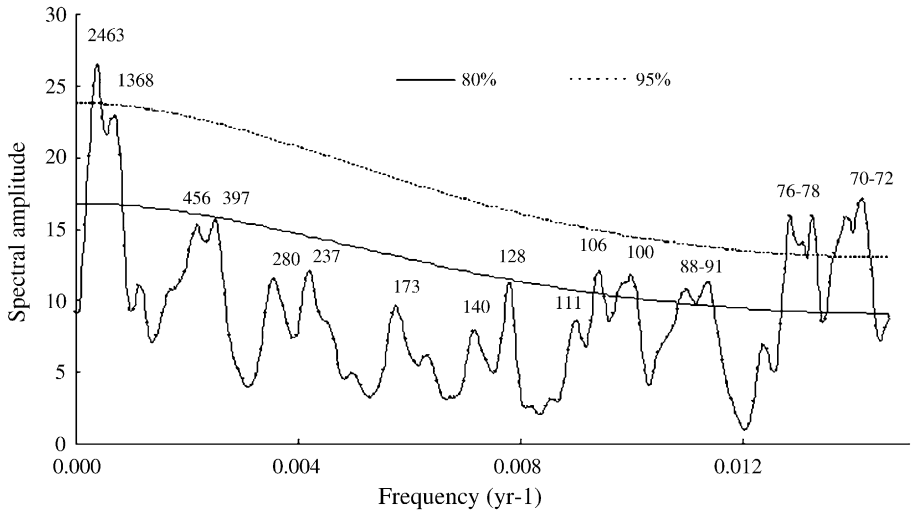

Fig. 9. Frequency analysis of Core PC-6 mean grain-size record for the entire samples. Parameters used are: nsim=1500, n50=4, iWin=2 and others are defaulted. Real and dashed lines are confident levels of 80% and 95%, respectively.

years shows that statistical 65–70-year oscillation existed in the North Atlantic Ocean and its bounding Northern Hemisphere continents. The authors thought the 65–70-year oscillation was neither global nor pan-oceanic. The most probable cause of this oscillation is an internal oscillation of the atmospheric-ocean system (Schlesinger and Ramankuty, 1994). The analysis of ice core and tree ring data from five regions of western China in last 300 years showed a significant quasi-70-year cycle of dry and wet climatic changes (Li et al., 2003). The 70–72-year cycle was significantly inferred by Core PC-6 and Jinchuan peat $\delta^{13}C$ (Hong et al., 2001). This cycle also exists in the change of the Indian Monsoon (Agnihotri et al., 2002) and appears to be of solar origin, supporting the hypothesis of solar control on the Indian monsoon on a multi-decadal time scale, which is different from the result of Schlesinger and Ramankuty (Schlesinger and Ramankuty, 1994). Marcus (2004) Thus, the coherence between the secular variation curves of the mean grain-size of Core PC-6 and the number of sunspots – together with spectral analyses – suggest that the EAM is forced by sun irradiance. Because the absolute changes in solar intensity over the range of decades to millennia are small (Flige and Solanki, 1999) and the influence of the solar flux on climate is not well established, it is unclear how solar variability affects the monsoon. One possible reason is that the reducing solar irradiance leads to changes of atmospheric or oceanic circulation, which could cause an increasing temperature difference between continents and oceans during winter times, and resulting in a strengthening of the EAWM.

6. Conclusions

1. The fine population of the upper section of Core PC-6 is transported by the ECS winter coastal current. Its mean grain-size is a good proxy of the EAWM and becomes magnified when the EAWM strengthens. A high-resolution record of the EAWM during recent 8 kyr is reconstructed by using the changes of grain-size of cores from the mud area in the inner shelf of the ECS.
2. Comparison between the change in the number of sunspots and the high-resolution record of the EAWM during recent 8 kyr shows fewer sunspots resulted in the EAWM strengthening. The high correlation between them shows that inner relationship exists between the EAWM and sun irradiance.
3. The EAWM, EASM and India Monsoon share concurrent cycles during the timeframe, which agrees with the changes of sun irradiance. It can be concluded that sun irradiance is one of the primary controls on centennial- to decadal-scale changes of the EAWM and EASM.

Acknowledgements

We thank Prof. Harry Elderfield at the Department of Earth Sciences, University of Cambridge, for giving constructive suggestions for the first manuscript. We also express our thanks to Dr. Alexander Schimanski, at the Institute of Geosciences, University of Kiel, and another anonymous reviewer for giving good advice for revisions. This research was sponsored by National

Science Foundation of China (No. 40576032), An Innovation Foundation from Institute of Oceanology, Chinese Academy of Sciences (CAS) (No. L6102281), K. C. Wang Postdoctoral Fellowship from CAS (No. 20040921123415), Key Laboratory of Marginal Sea Geology, South China Sea Institute of Oceanology (SCSIO), CAS (No. MSGL0507), the CAS Pilot Project of the National Knowledge Innovation Program (No. KZCX3-SW-220), China Postdoctoral Science Foundation (No. 2005037177), Doctor Foundation of SCSIO, CAS (No. 50601-65), and China 863 Project (No. 2004AA616090).

References

Agnihotri, R., Dutta, K., Bhushan, R., Somayajulu, B.L.K., 2002. Evidence for solar forcing on the Indian monsoon during the last millennium. Earth and Planetary Science Letters 198, 521–527.

An, Z.S., Kukla, G., Porter, S.C., Xiao, J.L., 1991. Magnetic susceptibility evidence of monsoon variation on the Loess Plateau of central China during the last 130,000 years. Quaternary Research 36, 29–36.

Bond, G., Showers, W., Cheseby, M., Lotti, R., Almasi, P., deMenocal, P., Priore, P., Cullen, H., Hajdas, I., Bonani, G., 1997. A pervasive millennial-scale cycle in north Atlantic Holocene and glacial climates. Science 278, 1257–1266.

Boulay, S., Colin, C., Trentesaux, A., Pluquet, F., Bertaux, J., Blamart, D., Buehring, C., Wang, P., 2002. Mineralogy and sedimentology of Pleistocene sediments on the South China Sea (ODP Site 1144). In: Prell, W.L., Wang, P., Blum, P., Rea, D.K., Clemens, S.C. (Eds.), Proceedings of the Ocean Drilling Program Scientific Results, pp. 1–21.

Chang, C.P., Lau, K.M., 1980. Northeasterly cold surges and near equatorial disturbances over the winter MONEX during December 1974, Part II: Planetary scale aspects. Monthly Weather Reviews 108, 298–312.

Chen, B.X., Zhu, J.G., Lou, H.B., 1991. Monsoons Over East Asia. Meteorology Press, Beijing (in Chinese).

Chu, P.S., Parks, S.U., 1984. Regional circulation characteristics associated with a cold surge event over East Asia during winter MONEX. Monthly Weather Reviews 112, 955–965.

Dansgaar, W., Johnsen, S.J., Clausen, H.B., Dahl-Jensen, N., Gundestrup, N., Hammer, C.U., 1984. North Atlantic climatic oscillations revealed by deep Greenland ice cores. Climate Progress and Climate Sensitivity 29, Geophysical Monographs, pp. 288–298.

Ding, Y.H., 1996. Study on the test of the South China Sea Monsoon and the East China Monsoon. The Leading Edge and Prospect of Modern Atmospheric Science, Beijing, pp. 43–46 (in Chinese).

Ding, Z.L., Liu, T.S., Rutter, N.W., Yu, Z.W., Guo, Z.T., Zhu, R.X., 1995. Ice-volume forcing of East Winter Monsoon variation in the past 800,000 years. Quaternary Research 44, 149–159.

Flige, M., Solanki, S.K., 1999. The solar spectral irradiance since 1700. Geophysical Research Letters 26, 2465–2468.

Gao, S., Collins, M., 1998. The grain-size trend of sediments and dynamics of marine sediments. Funds of Chinese Sciences 4, 241–246 (in Chinese).

Gu, G.C., Hu, F.X., Zhang, Z.T., 1997. The sediment source and development mechanics of the muddy coast in the East Zhejiang (in Chinese with English abstract). Donghai Marine Science 15 (3), 1–12 (in Chinese with English abstract).

Guo, Z.G., Yang, Z.S., Lei, K., Qu, Y.H., Fan, D.J., 1999. Seasonal Variation of the sedimentary dynamic processed for the mud area in the northern East China Sea. Journal of Ocean University of Qingdao 29 (3), 507–513.

Hong, Y.T., Wang, Z.G., Jiang, H.B., Lin, Q.H., Hong, B., Zhu, Y.X., Wang, Y., Xu, L.S., Leng, X.T., Li, H.D., 2001. A 6000-year record of changes in drought and precipitation in northeastern China based on a $\delta^{13}C$ time series from peat cellulose. Earth and Planetary Science Letters 185, 111–119.

Hori, K., Saito, Y., Zhao, Q., Wang, P., 2002. Evolution of the coastal depositional systems of the Changjiang (Yangtze) River in response to late Pleistocene–Holocene sea-level changes. Journal of Sedimentary Research 72 (6), 884–897.

Hu, D.X., Yang, Z.S., 2001. The Key Process of Marine Fluxes in East China Sea. Ocean Press, Beijing (in Chinese).

Jian, Z., Wang, P., Saito, Y., Wang, J., Pflaumann, U., Oba, T., Cheng, X., 2000. Holocene variability of the Kuroshio current Trough, northwestern Pacific ocean. Earth and Planetary Science Letters 184 (1), 305–319.

Li, C., Chen, Q., Zhang, J., Yang, S., Fan, D., 2000. Stratigraphy and paleoenvironmental changes in the Yangtze Delta during the late Quaternary. Journal of Asian Earth Sciences 18 (4), 453–469.

Li, Y.L., Xu, Y., Qian, W.H., 2003. Dry and wet climate changes of western china in recent 300 years. Plateau Meteorology 22 (40), 371–376 (in Chinese with English abstract).

Liu, J.P., Milliman, J.D., 2004. Reconsidering melt-water pulses 1A and 1B: global impacts of rapid sea-level rise. Journal of Ocean University of China 3 (3), 183–190.

Liu, J.P., Milliman, J.D., Gao, S., Cheng, P., 2004. Holocene development of the Yellow River's subaqueous delta, North Yellow Sea. Marine Geology 209, 45–67.

Liu, J.P., Xu, K.H., Li, A.C., Milliman, J.D., Velozzi, D.M., Xiao, S.B.,Yang, Z.S., (in press). Flux and fate of Yangtze River sediment delivered to the east China sea. Geomorphology.

Marcus, P.S., 2004. Prediction on a global climate change on Jupiter. Nature 428, 723–726.

McCave, I.N., Magnighetti, B., Robinson, S.G., 1995. Sortable silt and fine sediment size-composition slicing: parameters for palaeocurrent speed and palaeoceanography. Palaeoceanography 10, 593–610.

McCave, I.N., Manighetti, B., Beveridge, N.A.S., 1995. Circulation in the glacial North Atlantic inferred from grain-size measurements. Nature 374, 149–151.

Meff, U., Burns, S.J., Mangini, A., Mudelsee, M., Fleitmann, D., Matter, A., 2001. Strong coherence between solar variability and the monsoon in Oman between 9 and 6 kyr ago. Nature 411, 290–293.

Milliman, J.D., Meade, R.H., 1983. World-wide delivery of river sediment to the oceans. Journal of Geology 91, 1–21.

Milliman, J.D., Qin, Y.S., Park, Y.A., 1989. Sediments and sedimentary processes in the Yellow and East China Seas. In: Taira, A., Masuda, F. (Eds.), Sedimentary Facies in the Active P1ate Margin. Terra Scientific Publishing Company, Tokyo, pp. 233–249.

Moerz, T., Wolf-Welling, T.C.W., 2001. Data report: fine-fraction grain-size distribution data and their statistical treatment and relation to processes. Site 1095 (ODP Leg 178, Western Antarctic Peninsula). In: Barker, P.F., Ramsay, A.T.S. (Eds.), Proc. ODP, Sci. Results, pp. 1–27.

Prins, M.A., Weltje, G.J., 1999. End-member modeling of siliciclastic grain-size distributions: the late Quaternary record of eolian and fluvial sediment supply to the Arabian Sea and its paleoclimatic

significance. In: Harbaugh, J., Watney, L., Rankey, G., Slingerland, R., Goldstein, R., Franseen, E. (Eds.), Numerical experiments in stratigraphy: recent advances in stratigraphic and sedimentologic computer simulations. SEPM (Society for Sedimentary Geology) Special Publication, pp. 91–111.

Prins, M.A., Postma, G., Cleveringaa, J., Crampb, A., Kenyonc, N.H., 2000a. Controls on terrigenous sediment supply to the Arabian Sea during the late Quaternary: the Indus Fan. Marine Geology 169, 327–349.

Prins, M.A., Postma, G., Weltje, G.J., 2000b. Controls on terrigenous sediment supply to the Arabian Sea during the late Quaternary: the Makran continental slope. Marine Geology 169, 351–371.

Qin, Y.S., Zhao, Y.Y., Chen, L.R., Zhao, S.L., 1987. Geology of the East China Sea. Science Press, Beijing (in Chinese).

Rea, D.K., Hovan, S.A., 1995. Grain-size distribution and depositional processes of the Mineral component of abyssal sediments: lessons from the North Pacific. Paleoceanography 12, 251–258.

Saito, Y., Yang, Z., Hori, K., 2001. The Huanghe (Yellow) River and Changjiang (Yangtze) River deltas: a review on their characteristics, evolution and sediment discharge during the Holocene. Geomorphology 41, 219–231.

Schlesinger, M.E., Ramankuty, N., 1994. An oscillation of global climate system of period 65–70 years. Nature 367, 723–726.

Schulz, M., Mudelsee, M., 2002. REDFIT: Estimating red-noise spectra directly from unevenly spaced paleoclimatic time series. Computers and Geoscience 28 (3), 421–426.

Solanki, S.K., Usoskin, I.G., Kromer, B., Schüssler, M., Beer, J., 2004. Unusual activity of the Sun during recent decades compared to the previous 11,000 years. Nature 431, 1084–1087.

Stephen, C.P., An, Z.S., 1995. Correlation between climate events in the north Atlantic and China during the last glaciation. Nature 375, 305–307.

Stuiver, M., Braziunas, T., 1993. Sun, ocean, climate and atmospheric $^{14}CO2$: an evaluation of causal and spectral relationships. Holocene 3 (4), 289–305.

Stuiver, M., Braziunas, T., Becker, B., Kromer, B., 1991. Climate, solar, oceanic and geomagnetic influence on Late-Glacial and Holocene atmospheric $^{14}C/^{12}C$ change. Quaternary Research 35, 1–24.

Stuiver, M., et al., 1998. INTCAL98 Radiocarbon age calibration 24,000~0 cal aBP. Radiocarbon 40, 1041–1083.

Stuut, J.-B.W., Prins, M.A., Schneider, R.R., Weltje, G.J., Jansen, J.H.F., Postma, G., 2002. A 300-kyr record of aridity and wind strength in southwestern Africa: inferences from grain-size distributions of sediments on Walvis Ridge SE Atlantic. Marine Geology 180, 221–233.

Su, J., 2001. A review of circulation dynamics of the coastal oceans near china. Acta Oceanologica Sinica 23 (4), 1–16 (in Chinese with English abstract).

Su, Y.S., Li, F.Q., Ma, H.L., Qian, Q.Y., 1989. Formation and seasonal changes of the northern bottom cold water in the East China Sea. Oceanologia et Limnologia Sinica 19 (1), 1–14 (in Chinese with English abstract).

Sun, X.G., Fang, M., Huang, W., 2000. Spatial and temporal variations in suspended particulate matter transport on the Yellow and East China Sea shelf. Oceanologia et Limnologia Sinica 31 (6), 581–587 (in Chinese with English abstract).

Sun, D., Bloemendal, J., Rea, D.K., Vandenberghe, J., Jiang, F., An, Z., Su, R., 2002. Grain-size distribution function of polymodal sediments in hydraulic and Aeolian environments, and numerical partitioning of the sedimentary components. Sedimentary Geology 152, 263–277.

Sun, Y.B., Gao, S., Li, J., 2003. Primary analysis on the sensitive grain-size of terrigenous sediment to environments in marginal sea. Chinese Science Bulletin 48 (1), 83–87.

Sun, D., Jan, B., Rea, D.K., An, Z., Jef, V., Lu, H., Su, R., Liu, T., 2004. Bimodal grain-size distribution of Chinese loess, and its palaeoclimatic implications. Catena 55, 325–340.

Trewartha, G.T., 1981. The Earth's Problem Climate. Univ. Wisconsin Press, Madison.

Wang, L., Sarnthein, M., 1999. Holocene variations in Asian Monsoon Moisture: a bidecadal sediment record from the South China Sea. Geophysical Research Letters 26 (18), 2889–2892.

Wang, Y., Cheng, H., Edwards, R.L., He, Y., Kong, X., An, Z., Wu, J., Kelly, M.J., Dykoski, C.A., Li, X., 2005. The Holocene Asian monsoon: links to solar changes and North Atlantic climate. Science 308, 854–857.

Winkler, M.G., Wang, P.K., 1993. The Late Quaternary vegetation and climate of China. In: Wright Jr., H.E., et al., (Eds.), Global Climates Since the Last Glacial Maximum. University of Minnesota Press, Minnesota, pp. 221–264.

Xiao, S.B., Li, A.C., 2005. A study on environmentally sensitive grain-size population in inner shelf of the East China Sea. Acta Sedimentologica Sinica 23 (1), 27–34 (in Chinese with English abstract).

Xiao, S.B., Li, A.C., You, Z., Chen, L., 2005a. Provenance of the recent 2 ka mud off the Min-zhe provinces coast. Acta Sedimentologica Sinica 23 (2), 280–286 (in Chinese with English abstract).

Xiao, S.B., Li, A.C., Jiang, F.Q., Li, T.G., Huang, P., Xu, Z.K., 2005b. Recent 2000-year geological records of mud in the inner shelf of the East China Sea and their climatic implications. Chinese Science Bulletin 50 (5), 466–471.

Xiao, S.B., Li, A.C., Chen, M.H., Liu, J.P., Jiang, F.Q., Li, T.G., Xie, Q., Xiang, R., Chen, Z., 2005c. Recent 8 ka mud records of the East Asian Winter Monsoon from the inner shelf of the East China Sea. Earth Science-Journal of China University of Geosciences 30 (5), 573–581 (in Chinese, with English abstract).

Yasunari, T., Seki, Y., 1992. Role of the Asian Monsoon on the interannual variability of the global climate system. Journal of the Meteorological Society of Japan 70, 177–189.

Zhang, J.C., Lin, Z.G., 1992. Climate of China. Wiley, New York.

Zhu, R.L., 2001. Biography of the Yangtze River. Heibei University Press, Baoding, p. 377 (in Chinese).